International Journal of Terrestrial Heat Flow and Applied Geothermics
VOL. 4, NO. 1 (2021); P. 140-147.
ISSN: 2595-4180
DOI: https://doi.org/10.31214/ijthfa.v4i1.63

IJTHFA
http://ijthfa.com/

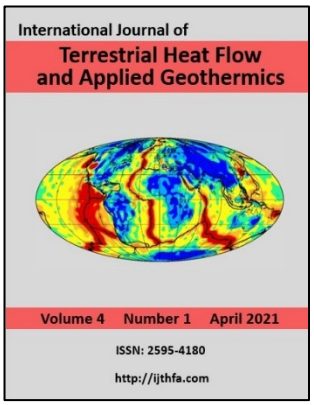

Keywords
Geothermal evidences,
Climate Changes of recent past,
Amazon region,
Brazil.

Received: November 15, 2020

Accepted: February 24, 2021

Published: April 01, 2021

Inversion results appended with estimates from vegetation changes in assessment of Ground Surface Temperatures for the Amazon Region, Brazil

Valiya Hamza[2], Fabio Vieira[2], Suze Guimaraes[2], Elizabeth Pimentel[1]

[1] Department of Physics, Federal University of Amazonas, Humaita, Brazil.
[2] Department of Geophysics, National Observatory, Rio de Janeiro, Brazil.

Email address
hamza@on.br (V. Hamza)
Corresponding author

Abstract

Estimates have been made of ground surface temperature (GST) variations for 25 localities in the region of Manaus (province of Amazon in Brazil) making use of both forward and inverse models. The work is based on analysis of borehole temperature logs as well as remote sensing data concerning changes in vegetation cover. Results of functional space inversion (FSI) of borehole temperature data reveal the occurrence of a cooling event, with a decrease in temperature of slightly less than 1°C, for the period of 1600 to 1850 AD. This episode coincides roughly with the period of "little ice age" in the southern hemisphere. It was followed by a warming event, with magnitudes varying from 2 to 3°C, that lasted until recent times. Integration of these results with estimates based on changes in normalized index of vegetation cover (NVDI) of the last decade points to continuation of climate warming over the last decade. This event is found to be prominent in areas of deforestation in central parts of the Amazon region.

1. Introduction

Ground Surface Temperature (GST) variations arising from climate changes are known to penetrate near surface layers of the earth's crust (Birch, 1948; Cermak, 1971; Beck, 1982). Thermal regime at shallow depths are thus characterized by the presence of down-going climate-related temperature signals superimposed on temperature variations arising from outflow of geothermal heat (Lachenbruch et al., 1986; Cavalcanti and Hamza, 2001; Hamza, 1991). The temperature logs of boreholes are thus capable providing information about past climatic changes. Pioneering studies aimed at extracting information on past climate changes, making use of borehole temperature data from Brazil, was carried out by Hamza (2007) and Hamza and Vieira (2011). A summary of long-term changes in the southern and eastern parts reveals a gradual cooling trend over the last several centuries, with magnitudes varying not more than 2°C. Another notable trend are indications of an increase of 1 to 3°C in GST variation since 1850. More recently, climate change events in the Amazon region have been studied in some detail (Araujo, 1999; Oliveira et al., 2006; Hamza, 2007; Pimentel and Hamza, 2012). In the present work, we examine features in temperature logs of boreholes in the western parts of Amazon region indicative of past climate changes. The locations of boreholes are indicated in the map of Figure 1. Also indicated in this map are locations (red dots) of oil wells with measurements of bottom-hole temperatures (BHT).

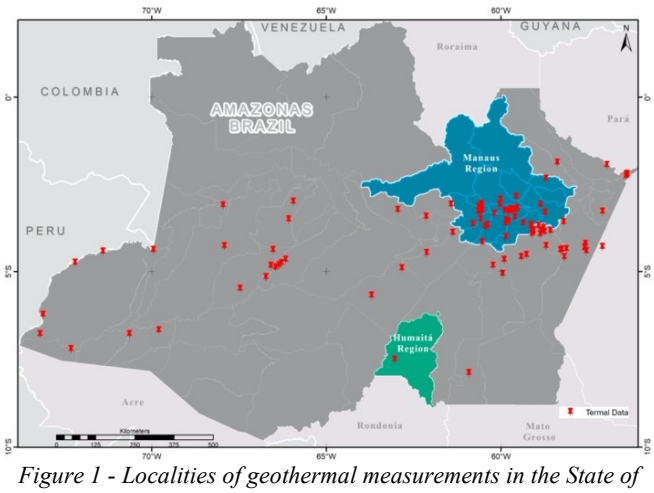

Figure 1 - Localities of geothermal measurements in the State of Amazonas.

2. Characteristics of Borehole Data

Three different sets of observational data sets of borehole temperature logs were considered in the present work. The earliest is that reported in the work of Araujo (1999) for five shallow boreholes in the area of Manaus, located in the central parts of the Amazon region. A summary of this data is presented in Table 1. The third column of this table indicates the depth intervals of temperature measurements. Values of temperature gradients are given in the last column.

Table 1 - Temperature log data reported by Araujo (1999). DI - depth interval of measurements; G – temperature gradient.

Well	Lon / Lat	DI (m)	G (ºC/km)
P1	60.17 / 3.11	60 – 125	25.0
P2	60.11 / 3.11	60 - 125	22.4
P3	60.02 / 3.11	60 - 90	20.0
P4	60.02 / 3.11	70 - 120	15.0
IA-1a	60.02 / 3.11	59 – 85	14.31
IA-1b	60.02 / 3.11	0 - 60	-
IA-1c	60.02 / 3.11	39 - 110	16.37

The vertical distribution of temperature data listed in Table 1 is illustrated in Figure 2. At depths greater than approximately 60m temperature variations follow linear trends, indicative of local thermal gradients. However, these profiles do not indicate curvatures typical of climate induced changes.

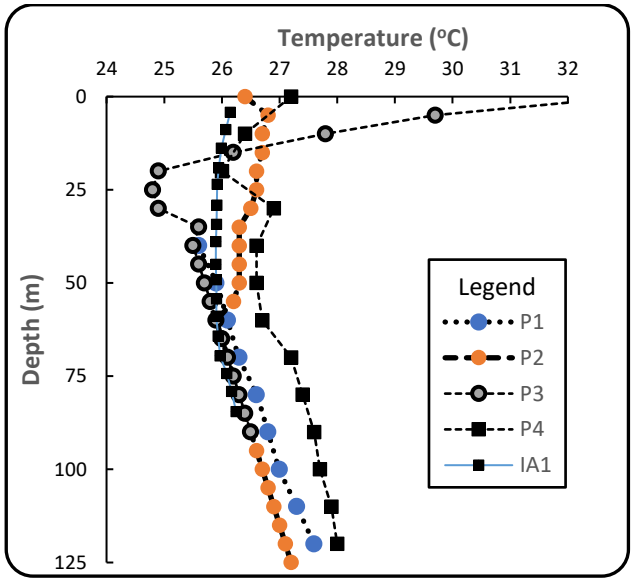

Figure 2 - Temperatures in boreholes in the region of Manaus (Araujo, 1999).

The data in Table 2 refer to temperature log data reported in the work of Olivera et al. (2006). Most measurements were carried out in sites located in the northern parts, adjacent to the urban area of Manaus. A notable feature is the presence of low gradients at shallow depths of less than 200 meters. At larger depths inferred values of temperatures indicate larger gradients with values in the range of 23 to 25 ºC/km.

Table 2 - Summary of temperature log data reported by Oliveira et al. (2006) for regions adjacent to the urban area of Manaus. For abbreviations see Table 1.

Well	Lat / Lon	D. I. (m)	G (ºC/km)
P1	3.24/ 60.74	130 – 200 205 - 295	4.0 24.68
P2	3.09/ 60.85	75 – 145 150 - 205	9.4 25.9
P3	3.085/ 60.88	75 – 170 170 - 260	3.93 23.99
P4	3.00/ 60.86	65 – 160 165 - 210	7.46 24.85
P5	3.15/ 60.73	60 – 155 160 - 210	6.71 24.24
P6	3.11/ 60.63	60 – 165 165 - 200	5.05 22.81
P7	3.045/ 60.85	95 – 135 140 - 180	3.63 23.67
P8	3.21/ 60.79	120 – 185 190 - 245	7.75 23.88
P9	3.16/ 60.67	85 – 180 185 - 255	3.5 24.41
P10	3.15/ 60.75	60 – 130 135 - 170	1.22 25.1
P11	3.22/ 60.81	85 – 145 150 - 185	1.58 24.60

The vertical distribution of temperatures in boreholes of Table 2 are illustrated in Figure 3. Most of the profiles indicate curvatures typical of climate induced changes at depths less than 100 meters. At depths greater than 100 meters, temperature distributions are characterized by near linear variations. The gradient values are however relatively low, in the range of 10 to 15ºC/km. This feature has been considered as indicating absence of climate related variations at deeper levels. At depths larger than 150 meters the gradient values are higher, in the range of 22 to 28ºC/km. These are related to changes in thermal conductivity of deeper formations.

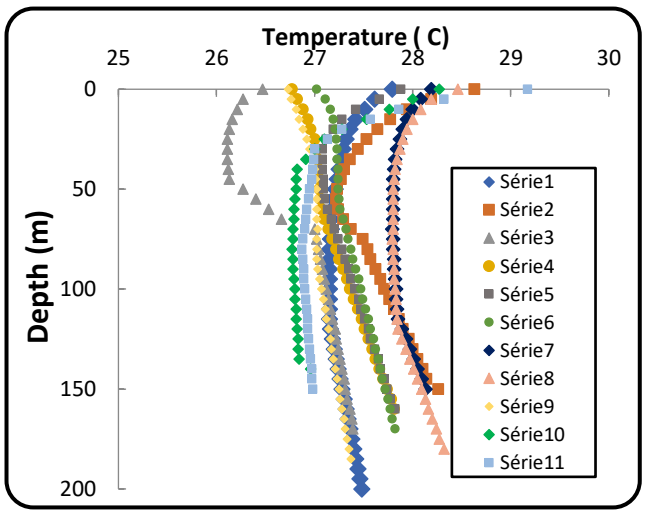

Figure 3 - Vertical distribution of temperatures in the central district of Manaus (Oliveira et al., 2006).

Table 3 refers to temperature logs reported in the work of Pimentel and Hamza (2012). Measurements were carried out in nine wells located in the urban area of Manaus. A notable

feature is the presence of relatively low gradients (most of them < 2ºC/km), at depths generally less than 100 meters. Pimentel and Hamza (2011) interpreted such low values as the consequence of regional scale down flow of ground waters. The model proposed by Ramey (1962) was employed in determining down flow velocities, estimated to be less than $2x10^{-7}$ m/s.

Table 3 - Data reported by Pimentel and Hamza (2012). DI – Depth interval of temperature measurement; V - velocity of ground water flow.

Bore hole Location	Lat. / Lon	DI (m)	G (ºC/km)	V (10^{-7} m/s)
Amazonino Mendes	3.0361/ 59.9428	80-210	0.48	1.2
Bola Coroado	3.0894/ 59.9734	80-145	0.06	1.0
Coroado III	3.0926/ 59.9885	80 -160	0.37	2.0
Francisca Mendes	3.0147/ 59.9724	80-190	0.38	1.3
Monte Sinai	3.0328/ 59.9987	105-215	1.78	1.3
Eduardo Braga	3.0122/ -59.9797	60-195	5.1	1.0
Eduardo Gomes	3.0450 60.0330	80-96	1.7	0.7
Vila Real	2.0234/ 59.9664	140-205	2.0	1.4
Presid. Figueredo	3.0020 59.9540	105-130	0.78	0.8

The vertical distribution of temperatures in boreholes of Table 3 are illustrated in Figure 4. Most of the temperature profiles indicate curvatures atypical of climate induced changes in depths less than 100 meters. At depths greater than 100 meters temperatures are constant which has been interpreted as indicative of significant down flows of groundwater.

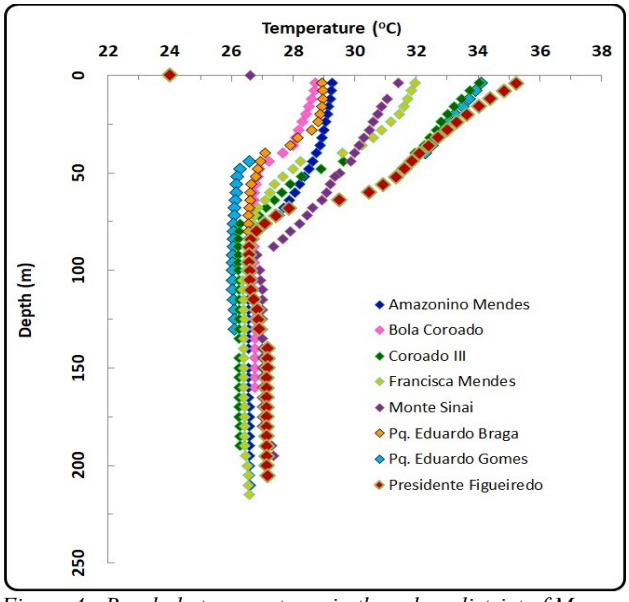

Figure 4 - Borehole temperatures in the urban district of Manaus (Pimentel and Hamza, 2012).

3. Forward Model Results

In the methodology of the present work, the near surface layer of earth is considered as a homogeneous medium where transport of heat is exclusively by solid-state conduction. In this forward modeling approach, it is customary to make a priori assumption as to the form of surface temperature variation. The theoretical curves that best fit the observational data set may then be used for determining the surface temperature history.

According to models discussed by Carslaw and Jaeger (1959), a simple analytical solution of standard heat conduction equation may be obtained by assuming a power law variation of surface temperature (T) with time (t):

$$v(0,t) = D\left(\frac{t}{t^*}\right)\frac{n}{2} \quad \text{for } 0 < t \le t^* \qquad (1)$$

where t^* is the duration of the climatic event and D the magnitude of the perturbation. Lachenbruch et al. (1986) pointed out that the value of n may be used to specify the form of temperature variation. For the initial condition ($t = 0$) given $v(z,0) = 0$, the solution is:

$$v(z,t) = D2^n\Gamma\left(\frac{n}{2}+1\right) i^n erfc\left(\frac{z}{\sqrt{4\alpha t^*}}\right) \qquad (2)$$

where α is the thermal diffusivity of the medium, Γ the gamma function, $i^n erfc$ the n^{th} integral of the complementary error function.

In studies aimed at extracting climate related information from borehole temperature logs it is normal practice to remove the component of temperature variation arising from deep heat flux. In many cases, temperature data from deeper parts of the borehole, which are relatively free of surface perturbations, provide a convenient means of determining the 'undisturbed' geothermal gradient. The residual temperature profile, obtained after subtracting that arising from the geothermal gradient, may be considered as containing climate related signals. Best fitting curves would then allow the determination of the model parameters. An example of this standard procedure is illustrated in the Figure 5. The results indicate that forward modelling for well 1 in Manaus is compatible with climate warming of 2.7ºC over the last 420 years.

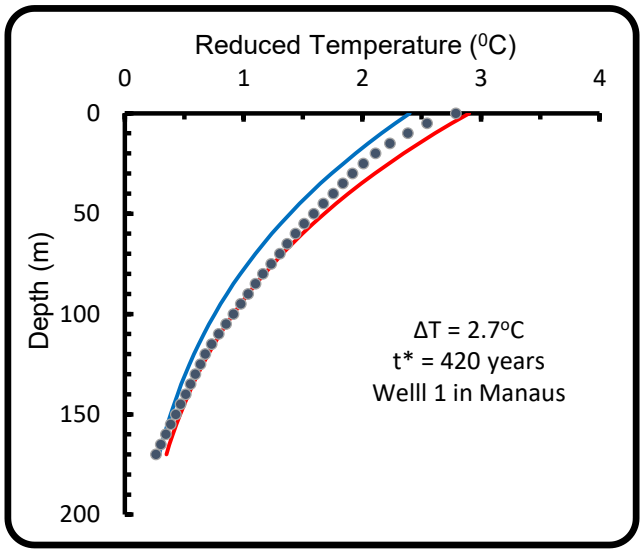

Figure 5 - Forward model fit to log data of hole 1 in the region of Manaus.

Log data for the upper parts of wells 2, 3, 5, 8, 10 and 11, reported in the work of Oliveira et al. (2006) also reveal similar curvatures. However, such features are limited to

depth intervals of less than 50 meters where uncertainty in observational data is large. This implies that thermal signals of climate changes at subsurface levels are not widespread in the neighboring areas of Manaus. It is also possible that, other near surface processes such as vegetation changes or ground water flows will have interfered with temperature distributions at shallow depths. Hence such data have been excluded from further analysis in this work. Log data for wells 4, 6, 7 and 9 revealed curvatures indicative of warming episodes, but again limited to shallow depths of less than 50 meters. Hence no attempts were made in presenting forward model results for these remaining wells. Log data for some wells reported in the work of Pimentel and Hamza (2012) have features indicative of down flow of groundwater at shallow depths. These were also considered as unsuitable for climate studies of the present work.

4. Inverse Model Results

In the inverse method, temperature history that best fit the data set is obtained as a posteriori result. The functional space inversion procedure suggested by Shen and Beck (1992) was adopted in the present work. For reasons of brevity we do not describe detailed descriptions of inverse models. In obtaining a stable solution in inverse models it is necessary to adopt a criterion for a weighted function that provide least square fit for uncertainties in data and model (S(m)):

$$S(m) = \frac{1}{2}(d - d_0)^t C_d^{-1}(d - d_0) + \frac{1}{2}(m - m_0)^t C_m^{-1}(m - m_0) \qquad (3)$$

where C_d e C_m are the operators of the covariances that describe the uncertainties in the observational data (d_0) and the a priori model parameters (m_0). Detailed descriptions of inverse models have been discussed in several recent works (Beltrami et al., 1995; Safanda, 1999)

In the present context, the discussion of the uses of inverse models is limited to results obtained for log data for four selected wells in the region of Manaus (Amazon, Brazil). Examples of the results obtained by the inversion procedure of Shen and Beck (1983) are illustrated in Figures 6, 7, 8 and 9, respectively for wells 1, 2, 5 and 8. Note that the inversion procedure are limited to data for the upper parts of logs. Analysis of data in the lower parts of temperature logs, reported by Oliveira et al. (2006) do not include intervals with relatively high temperature gradients.

The results illustrated in the set of illustrations of Figure 6 reveal several characteristics of GST changes in the region of Manaus. To begin with there are considerable similarities in climate changes derived for the different sites. This is understandable as the holes are not separated by large distances. Also, the depth range of data is incapable of identifying climate changes over times prior to 1300 years AD. During the period of approximately 1500 to 1850 there has been steady decline in surface temperatures with magnitudes less than 1°C. This cooling event coincides with the time interval of little ice ages reported for southern latitudes (Mann et al., 1998; Meyer et al., 2009).

This cooling event is followed by a climate warming episode that occurred during the period of 1850 and 1950. The warming event is characterized by an increase of about 2 to 3°C in GST. There are indications that the warming trend continued during the recent years since 1980. However, temperature log data from shallow depths are affected by short period near surface variations, making it difficult to deduce complete climate history of the last few decades.

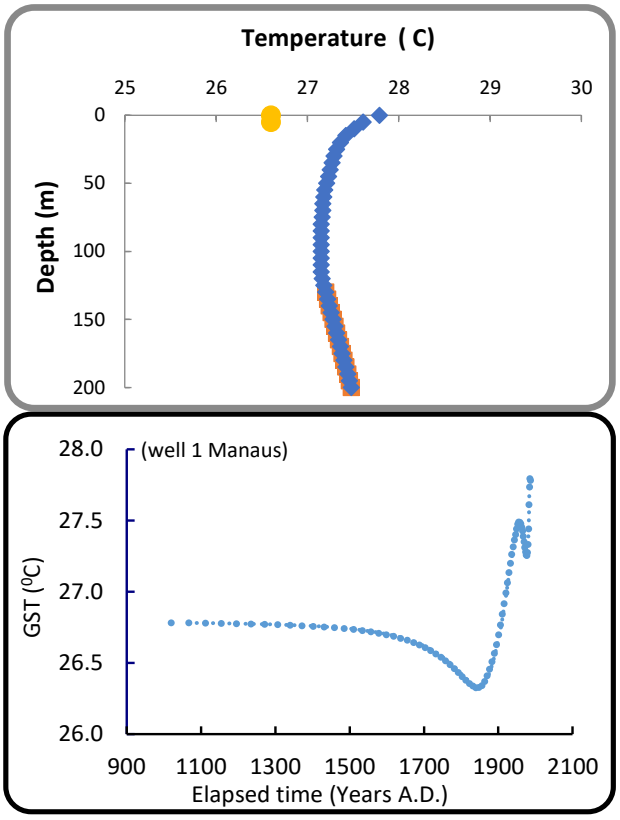

Figure 6 - Temperature distribution (upper panel) and GST variations (lower panel) calculated for the site of well 1.

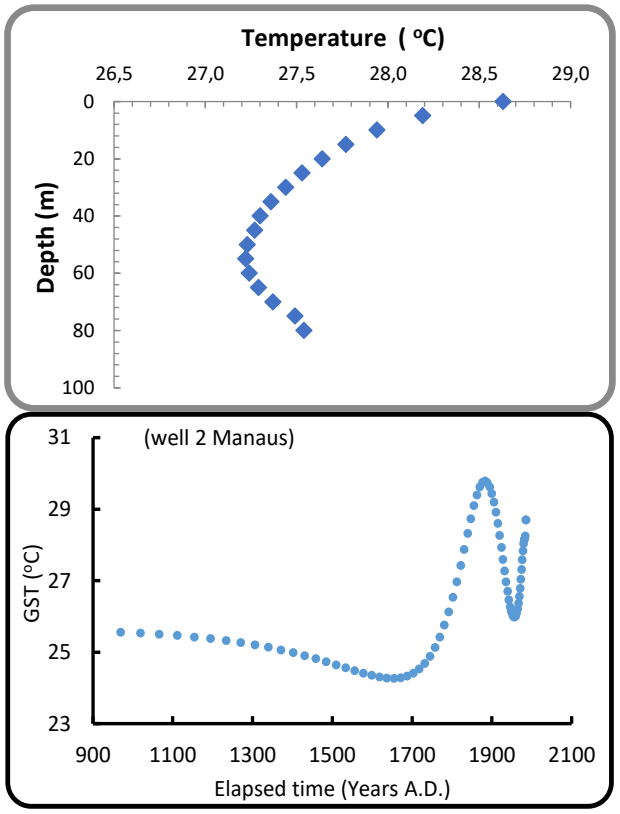

Figure 7 - Temperature distribution (upper panel) and GST variations (lower panel) calculated for the site of well 2.

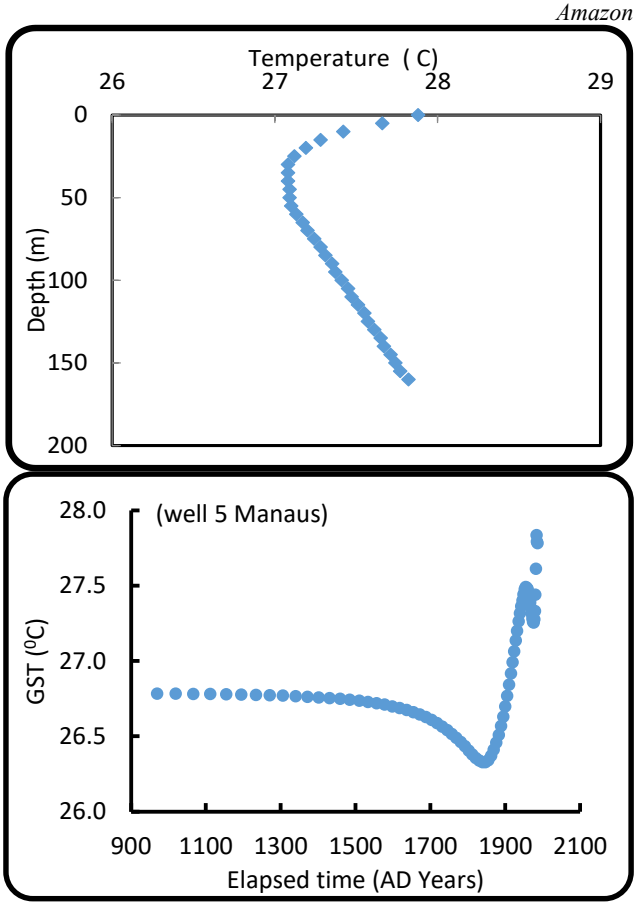

Figure 8 - Temperature distribution (upper panel) and GST variations (lower panel) calculated for the site of well 5.

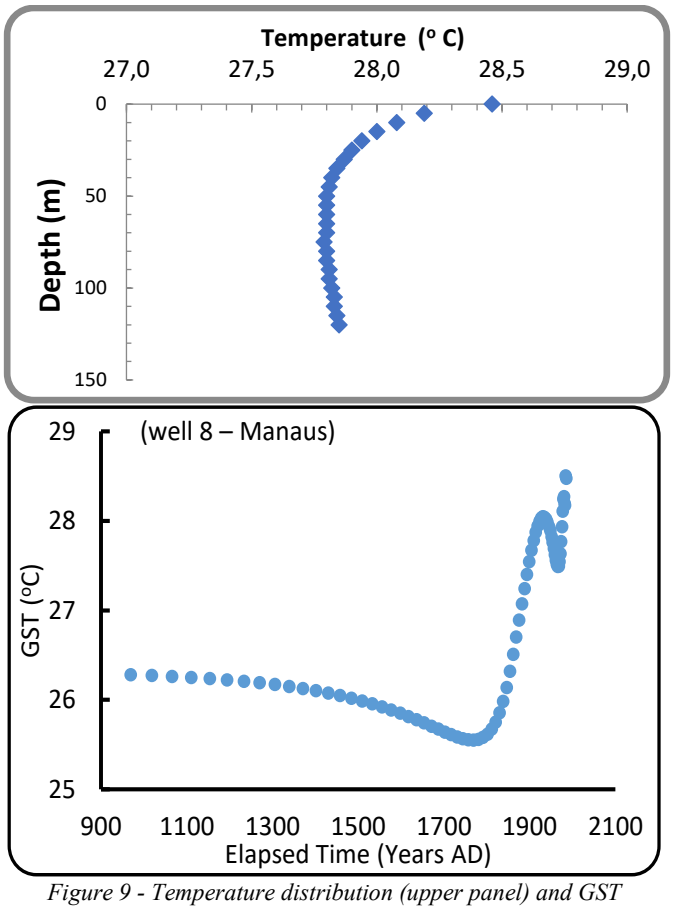

Figure 9 - Temperature distribution (upper panel) and GST variations (lower panel) calculated for the site of well 8.

5. GST Variations arising from Changes in Vegetation cover

A convenient method of tracing the GST history of the last few decades is to make use of available information on processes that have direct effect on surface temperatures, such as the vegetation cover. Empirical relations are available now that describe changes in vegetation cover and its effects on surface temperatures. Several studies have been carried out on the effect of vegetation cover on surface temperatures (see for example work by Matos and Silva, 2005). As an illustrative example, consider here results of multitemporal study reported by Caioni et al. (2017) for the southern part of the Amazon region. According to results of this study Amazon biome plays a strong role in local climate regulation. Also, anthropogenic uses of land cause significant changes in soil temperatures. The study of Caoini et al. (2017) refers to the area of Carlinda (Province of Mato Grosso). It examined the relationship of normalized differences in vegetation index (NDVI), using images of Landsat 5. According to authors of this work the indices were obtained from bands 3 and 4, referring to the mid-infrared and near infrared bands, respectively. To obtain the thermal level conversion has been performed in band 6 of digital values of temperatures. The results in their work indicate strong relationships between values of vegetation indices and soil temperatures. Maps of NDVI adapted from this work are presented in Figure 10 and illustrate the relation between vegetation cover and surface temperatures.

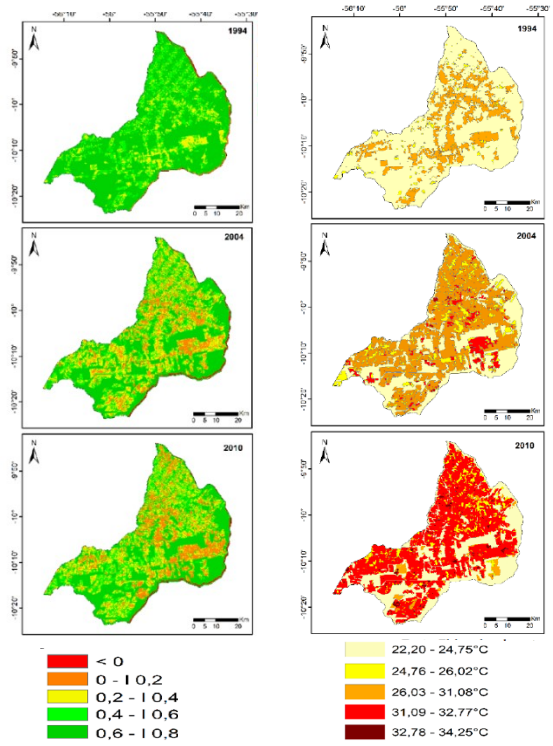

Figure 10 - Relationship between vegetation index (left panel) and land surface temperatures (right panel) for the southern parts of the Amazon region (Adapted from Caioni et al., 2007).

A more recent study was carried out by Guilherme et al. (2020) in the Coari area adjacent to the region of Manaus. In this latter work the surface albedo, which synthetically consists of the reflective power of a surface, was calculated according to the procedure described by Silva et al. (2016).

They argued that the forest has high radiation absorption power, and hence albedo can be an indicator of built-up areas or exposed soil. Hence use has been made of Normalized Difference Built-up Index (NBDI) proposed by Alhawiti and Mitsova (2016). The values of NVDI and NBDI were calculated using the relations:

$$NDVI = \frac{\rho_5 - \rho_4}{\rho_5 + \rho_4}$$

$$NDBI = \frac{\rho_6 - \rho_5}{\rho_6 + \rho_5}$$

Where ρ_4, ρ_5, and 6 are surface reflectance of bands 4, 5 and 6 of the Landsat 8, which correspond to the red near infra-red bands. The value of land surface temperature (LST) using the relation with calibration constants K_1 and K_2 and value of spectral radiance at the top of the atmosphere (W/m^{-2} srad^{-1} μm^{-1}) L_λ is:

$$LST = \frac{K_2}{\ln\left(\frac{K_1}{L_\lambda} + 1\right)} - 273.15$$

They reported a good linear relation between NBDI and land surface temperature (LST), illustrated in Figure 11.

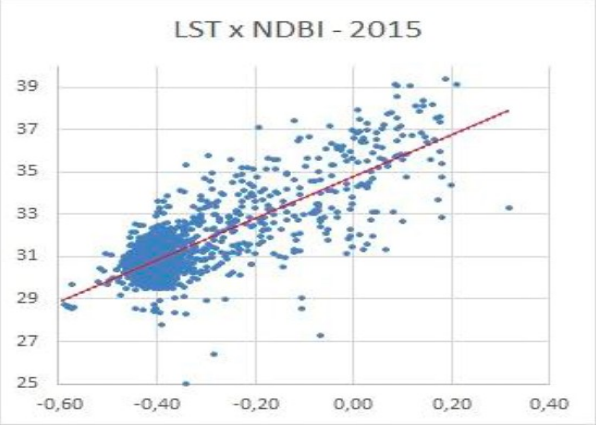

Figure 11 - Relationship between vegetation index NBDI and land surface temperatures (LST) for areas adjacent to the region of Manaus (Adapted from Guilherme et al., 2020).

Results of both studies indicate strong relationships between values of vegetation indices and soil temperatures. It is clear that the increase in anthropic use and reducing the extent of vegetation, has led to significant changes in NDVI and NDBI, which has been the main cause of the rise in surface temperatures.

6. Appending GST Variations derived from Inverse models with those Derived from indices of Changes in Vegetation Cover

In this section, we consider estimates of GST changes of the study area in Manaus, based on reported values of historic changes in vegetation cover. This allows integration of GST data from inversion of temperature logs with those derived from data on changes in vegetation cover. Consequently, it is possible to append GST history derived from inversion models with those for periods of changes in vegetation cover. As illustrative examples, consider the relevant data sets for sites of wells 1, 2, 5 and 8, illustrated in Figures 12a, 12b, 12c and 12d. In this set of figures, the blue dots indicate GST values derived from inversion model of Shen and Beck (1992). The line in red color indicates maximum estimates of GST derived from NDVI indices for vegetation changes. The small green line indicates values derived from lower limit for NVDI. The yellow triangle indicates the estimated range of GST variation associated with vegetation changes.

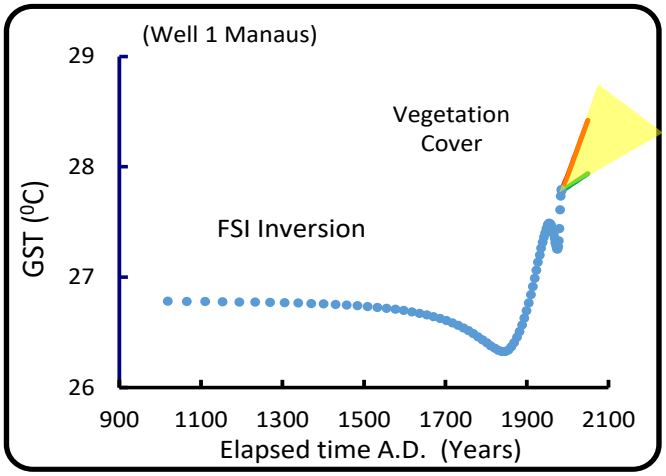

Figure 12a - GST variations derived from inverse model and index for vegetation cover at the site of well 1, Manaus.

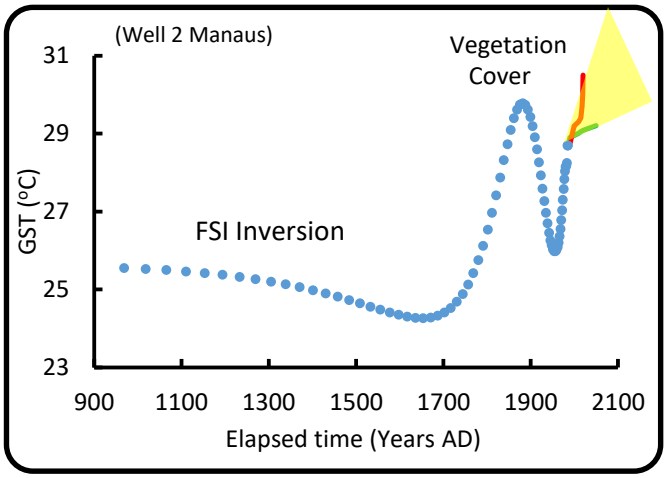

Figure 12b - GST variations derived from inverse model and index for vegetation cover at the site of well 2, Manaus.

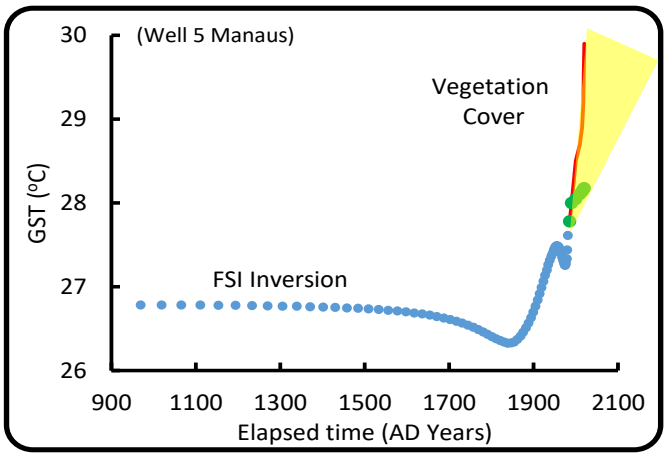

Figure 12c - GST variations derived from inverse model and index for vegetation cover at the site of well 5, Manaus.

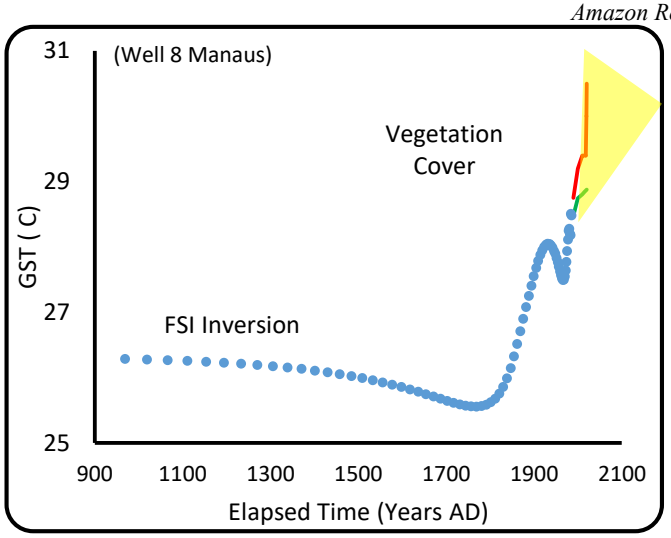

Figure 12d - GST variations derived from inverse model and index for vegetation cover, for site of well 8, Manaus.

7. Results and discussion

In this work, we have examined the natures of ground surface temperature variations for 25 localities in the district of Manaus located in the central parts of the province of Amazon (Brazil). The results obtained are based on analysis of borehole temperature logs as well as remote sensing data derived from changes in vegetation cover. According to results derived from inversion of functional space inversion (FSI) of borehole temperature data, the cooling event that occurred during the period of 1600 to 1850 AD was responsible for decrease of about 1ºC. This episode coincides roughly with the period of "little ice age" in the southern hemisphere. It is followed by a warming event, when temperatures increased by as much as 1 to 3ºC, that lasted until recent times. However, in accordance with results of the present work the most dramatic increase in surface temperatures of the study area took place in the last few years, a result of deforestation activities during the period of 2008 to 2020.

8. Acknowledgments

The first author of this work is recipient of a research scholarship (Process No. 306755/2017-3) granted by the National Research Council of Brazil (CNPq). The second author is Coordinator of the Department of Geophysics of the National Observatory (ON/MCTI). The third author is recipient of a post-doctoral scholarship (PNPD) at the Department of Geophysics of the National Observatory - ON/MCTI. The fourth author is a member of the faculty of science at Campus Humaitá of federal University of Amazonas. Project FAPEAM (Release 016/2014 – Protocol 062.01107/2017) provided support for environmental studies of the Amazon region using geothermal methods.

References

Alhawiti, R.H., Mitsova, D. 2016. Using Landsat-8 data to explore the correlation between Urban Heat Island and Urban Land uses. International Journal of Research in Engineering and Technology. 5, 457-466. DOI https://doi.org/10.15623/ijret.2016.0503083

Araujo, R.L.C. 1999. Contribution of Shallow geothermics in Environmental Studies (in Portuguese). EDUA, Manaus-AM, Brazil, 88 p.

Beck, A.E. 1982. Precision logging of temperature gradients and the extraction of past climate. In: M.L. Gupta (Editor), Terrestrial Heat Flow. Tectonoph.vsim., 83, I-1 I.

Beltrami, H., Jessop, A.M., Mareschal, J.C. 1995. Resolution of ground temperature histories inverted from borehole temperature data. Global and Planetary Change I I, 57-70.

Birch, F. 1948. The effects of Pleistocene climatic variations upon geothermal gradients, Am. J. Sci., 246, 729–760.

Caioni, C., Silva Neves, S.M.A., Seabra Junior, S., Neves, R.J. 2017. Multimedial analysis of the surface temperature of the municipality of Carlinda - Mato Grosso, Bol. Geogr., Maringá, 35(3), 26-40.

Cavalcanti, A.S.M., Hamza, V.M. 2001. Climate changes of the recent past in southern parts of Brazil (Abstract). Proceedings of the 7th International Congress of the Brazilian Geophysical Society, Salvador (BA), 1.

Carslaw, H.S., Jaeger, J.C. 1959. Conduction of Heat in Solids, 386pp, Oxford University Press, New York.

Cermak, V. 1971. Underground temperature and inferred climatic temperature of the past millennium, Palaeogrogr., Palaeoclimatol., Palaeoecol., 10, 1-19.

Guilherme, A.P., Sacardi, M., Biudes, M.S., Mota, D.S., Musis, C.R. 2020. Relationship between soil cover type and surface temperature. Online Journal Society and Nature, 32, 515-525, DOI 10.14393/SN-v32-2020-47462.

Hamza, V.M. 1991. Recent climate changes in the southern hemisphere: the geothermal evidence, Proceedings 2nd Congress of the Brazilian Geophysical Society, Salvador (BA), 971-973.

Hamza, V.M. 2007. Climate changes in the eastern segment of the Amazon region: inferences based on geothermal method (In Portuguese). Proceedings of the Israeli International Congress of Sociosphere of Amazon – CISA. V Amazoníada: Em defesa da Amazônia, vol 1, Belem-PA, Brazil, 9 pp.

Hamza, V.M., Vieira, F.P. 2011. Climate changes of the recent past in the South American continent: inferences based on analysis of borehole temperature profiles. In: Blanco J, Kheradmand H (eds) Climate change: geophysical foundations and ecological effects. Intech. In: http://www.intechopen.com. Accessed November 2, 113–136.

Lachenbruch, A.H., Sass, J.H., Marshall, B.V. 1986. Changing Climate: Geothermal Evidence from Permafrost in the Alaskan Artic, Science, 234, 689-696.

Mann, M.E., Bradley, R.S., Hughes, M.K. 1998. Global-scale Temperature Patterns and Climate Forcing Over the Past Six Centuries, Nature, 392, 779–787.

Matos, A.F.D., Silva, E.K. 2005. Detecção de mudanças na cobertura vegetal na cidade de Manaus e seu entorno. Proceedings of the Brazilian Symposium on Remote Sensing, Goiânia, Brazil, INPE, 609-616.

Meyer, I., Wagner, S. 2009. The Little Ice Age in Southern South America: Proxy and Model Based Evidence. Past Climate Variability in South America and Surrounding Regions. Developments in

Paleoenvironmental Research, 14, 395–412. DOI 10.1007/978-90-481-2672-9_16. ISBN 978-90-481-2671-2.

Oliveira, F.N.M., Araujo, R.L.C., Carvalho, J.S., Silva, C.L. 2006. Inference on climate change in the region of Manaus (Am) using geothermal and meteorological data (in Portuguese). Brazilian Geophysical Journal, 24(2), 169-187.

Pimentel, E.T., Hamza, V.M. 2012. Indications of regional scale groundwater flows in the Amazon Basins: Inferences from results of geothermal studies Journal of South American Earth Sciences 37, 214 – 227.

Ramey, H.J. 1962. Wellbore heat transmission, J. Petrol. Technol., 14, 427-435.

Safanda, J. 1999. Ground surface temperature as a function of slope angle and slope orientation and its effect on the subsurface temperature field. Tectonophysics, 306(3–4), 367–375. DOI 10.1016/S0040-1951(99)00066-9

Shen, P.Y., Beck, A.E. 1983. Determination of surface temperature history from borehole temperature gradients. 7485-7493. First published: 10 September 1983.

Shen, P.Y., Beck, A.E. 1992. Palaeoclimate and heat flow density inferred from temperature data in the Superior Province of the Canadian Shield. Global and Planetary Change, 98, 143-165.

Silva, B.B., Braga, A.C., Braga, C.C., Oliveira, L.M.M., Montenegro, S.M.G.L., Barbosa Junior, B. 2016. Procedures for calculation of the albedo with OLI-Landsat 8 images: Application to the Brazilian semi-arid. Revista Brasileira de Engenharia Agrícola e Ambiental, 20(1), 3-8.